JOURNAL PRE-PROOF

This is an early version of the article, published prior to copyediting, typesetting, and editorial correction. The manuscript has been accepted for publication and is now available online to ensure early dissemination, author visibility, and citation tracking prior to the formal issue publication.

It has not undergone final language verification, formatting, or technical editing by the journal's editorial team. Content is subject to change in the final Version of Record.

To differentiate this version, it is marked as "PRE-PROOF PUBLICATION" and should be cited with the provided DOI. A visible watermark on each page indicates its preliminary status.

The final version will appear in a regular issue of *Archives of Acoustics*, with final metadata, layout, and pagination.

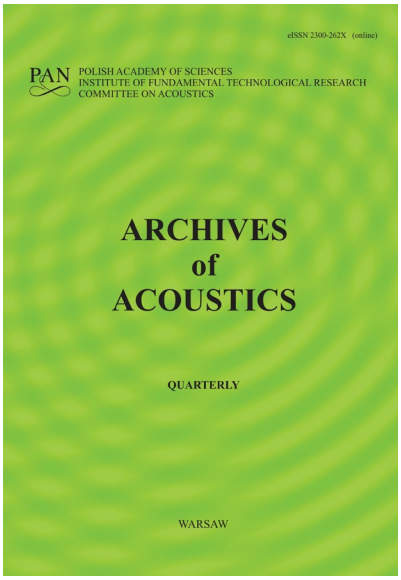

Title: Dispersion Characteristics of SH Waves in a Rotating Micro-structured Plate with Restrained Boundaries

Author(s): Mandeep Kaur, Satish Kumar, Vikas Sharma

DOI: https://doi.org/10.24423/archacoust.2026.4395

Journal: *Archives of Acoustics*

ISSN: 0137-5075, e-ISSN: 2300-262X

Publication status: In press

Received: 2025-12-13

Revised: 2026-04-03

Accepted: 2026-04-07

Published pre-proof: 2026-04-16

Please cite this article as:

Kaur M., Kumar S., Sharma V. (2026), Dispersion Characteristics of SH Waves in a Rotating Micro-structured Plate with Restrained Boundaries, *Archives of Acoustics*, https://doi.org/10.24423/archacoust.2026.4395

Dispersion Characteristics of SH waves in a Rotating Micro-structured Plate with Restrained Boundaries

Mandeep Kaur[1,*], Satish Kumar[2], and Vikas Sharma[3]

[1]Department of Mathematics, Thapar Institute of Engineering and Technology, Patiala, India, https://orcid.org/0009-0006-7380-5338

[2]Department of Mathematics, Thapar Institute of Engineering and Technology, Patiala, India, https://orcid.org/000000000000000

[3]Department of Mathematics, Lovely Professional University, Phagwara, India, https://orcid.org/000000000000000

[*]Corresponding Author e-mail: mkaur2_phd23@thapar.edu

Abstract

Shear horizontal (SH) waves in plates are elastic stress disturbances that propagate along bounded surfaces, with in-plane shear motion perpendicular to the propagation direction, influenced by physical, geometric, and boundary conditions. Due to their sensitivity to surface and subsurface defects, SH waves are widely employed in non-destructive testing (NDT), structural health monitoring (SHM), and material characterization. This study presents a theoretical investigation of SH-wave propagation in a rotating, microstructural elastic plate within the framework of Consistent Couple Stress Theory (CCST), incorporating elastically restrained boundary conditions. CCST introduces a characteristic length parameter to account for microstructural and size-dependent effects beyond classical elasticity. Restrained boundaries provide an intermediate model between idealized traction-free and rigid conditions, capturing realistic boundary behavior encountered in practical applications. An analytical dispersion relation is derived to examine the combined effects of boundary restraints, microstructural parameters, and rotational speed on SH-wave dispersion, with several special cases presented to validate the general formulation. Graphical results illustrate the influence of restraint stiffness, characteristic length, plate thickness, and rotation on SH-wave dispersion characteristics. The findings may offer valuable insights for the design of advanced sensing devices, the development of non-destructive evaluation techniques, and the analysis of seismic wave propagation in rotating geophysical layers.

Keywords: SH waves, Couple stress theory, Stiffness coefficients, Restrained boundary conditions, Dispersion curves, Rotating elastic plate.

1 Introduction

Waves propagating in rotating elastic plates have garnered considerable attention due to their relevance in both engineering and geophysical domains. Rotation introduces coriolis and centrifugal effects, which significantly alter the characteristics of wave motion—the coriolis force modifies wave trajectories and dispersion, while the centrifugal force shapes the equilibrium state. Understanding these influences may aid the design, analysis, and health monitoring of rotating systems in various engineering applications, where stress waves and vibrations can affect performance and reliability. In broader contexts, wave propagation in rotating layers may offer insights into seismic wave behavior, earthquake mechanics, and planetary dynamics and may also support the development of advanced sensing and non-destructive evaluation techniques. Bhuta and Jones (1963) established the foundational theoretical framework for analyzing the influence of uniform rotation on the propagation characteristics of elastic waves. Their study was the first to reveal the occurrence of elliptical polarization in wave motion, arising from the coriolis-induced coupling between displacement components. Further, Schoenberg and Censor explored plane wave solutions in rotating elastic solids in two (Censor, Schoneberg, 1973) and three-dimensions (Schoneberg, Censor, 1973). They have found that these waves do not exhibit purely shear or purely compressional characteristics and showed that the wave speeds are governed by the ratio of the rotational frequency of the medium to the angular frequency of the waves. Extensive studies have been conducted and documented in the literature (Advani, 1967; Advani, bulkeley, 1969; Bulkeley, 1973; Hashemi, Richard, 2001; Huang, Wang, 2001; Lamb, Southwell, 1921; Luo, Mote Jr., 2000; Nowinski, 1981; Southwell, 1922; Auriault, 2004; Kumar,Chawla, 2011; Yu,Yu, 1996) on wave propagation in different rotating elastic medias such as beams, disks, membranes, half-spaces and plates. Collectively, the findings demonstrate that rotation introduces strong coupling between different wave modes, profoundly influencing the stability, dispersion behavior, and dynamic response of the system. These insights significantly advance the understanding of wave–rotation interactions and the complex challenges associated with the analysis and design of rotating machinery.

Shear horizontal (SH) waves represent a fundamental class of elastic wave motion with broad applicability across geophysics, material science, structural health monitoring (SHM), and ultrasonic diagnostics. SH waves exhibit pure in-plane transverse particle motion perpendicular to the propagation direction, rendering them immune to mode conversion at free or bonded interfaces. This distinctive feature imparts high signal clarity, strong penetration through layered structures, and minimal dispersion, making SH waves exceptionally effective for non-destructive testing (NDT), surface acoustic wave (SAW) sensors and characterization of multilayered or anisotropic materials. When propagating in thin plates, SH waves are confined and guided by the plate boundaries, resulting in well-defined dispersion characteristics and enhanced sensitivity to surface, subsurface, and interfacial discontinuities. Casting and Hosten (2001) investigated the interaction between non-principal planes and the surrounding fluid in the propagation of quasi-shear horizontal (quasi-SH) modes, demonstrating that this coupling

enables the efficient generation and detection of such modes using air-coupled transducers in solid plates. Subsequently, Lee *et al.* (2010) introduced a novel technique for damage detection in plates based on focused SH waves, which significantly minimizes the number of transducers required while enhancing detection accuracy. Kuznetsov (2022) investigated the behavior of SH waves in functionally graded plates, incorporating bifurcation effects to enhance the understanding of their dynamic response and potential engineering applications. Shear horizontal (SH) waves in thin plates find extensive applications across various branches of engineering, serving numerous practical purposes such as material characterization, design and optimization of multilayered composite structures, and damping analysis in automotive, aerospace, and research industries (Kuznetsov, 2006; Phan *et al.*, 2019; Djeran-Maigre, Kuznetsov, 2014; Simonetti, Cawley, 2004; Jiangong, 2011).

In practical engineering applications, plates are often influenced by interactions with their surrounding environments and boundary surfaces, which significantly affect their dynamic and mechanical responses. However, capturing these complex interactions with full physical accuracy is often difficult; hence, simplified boundary idealizations are introduced to make the analysis tractable. The most common boundary conditions include the stress-free boundary, representing surfaces devoid of external constraints and the fixed (clamped) boundary, corresponding to fully restrained conditions where both displacement and rotation are restricted. To address the practical scenarios that lie between the two extreme boundary conditions, Mindlin (1960) introduced the concept of elastically restrained boundary conditions (ERBC) in the normal direction, modeling the boundary as exhibiting spring-like behavior governed by Hooke's law. Subsequently, Graff (2012) elaborated on these conditions and referred to them as mixed boundary conditions, which provide a continuous transition between stress-free and rigidly fixed boundaries. Moukhomodiarov *et al.* (2010) further examined this transition in a linear isotropic elastic layer, establishing a framework for intermediate boundary modeling. Expanding upon this foundation, Moukhomodiarov and Rogerson (2012a, 2012b) employed various analytical approaches to investigate the influence of ERBC on long-wave motion, and later extended their study to analyze long-wave dispersion phenomena in pre-stressed, incompressible elastic layers under ERBC (Moukhomodiarov, Rogerson, 2013). More recently, Paimushin and Gazizullin (2018) explored the effect of ERBC by introducing elastic spacers connecting the plate to a rigid frame, while kuznetsov (2015) analyzed the propagation characteristics of Lamb waves in elastic layers constrained by clamped and partially clamped boundaries.

Wave propagation is governed not only by the geometry and boundary conditions of the structure but also by the intrinsic material properties. In essence, the propagation behavior—depending on the medium and the nature of the wave is determined by the complex interplay among material characteristics, structural geometry, and boundary constraints. Although the behavior of shear-horizontal (SH) waves has been extensively studied in the context of rotational effects, it has not yet been comprehensively investigated within the framework of consistent couple stress theory (CCST). Hadjesfandiari and Dargush (2011) developed CCST

following the work of Mindlin and Tiersten (1962) and Koiter (1969) generalising and extending the classical theory of elasticity. It addresses the limitations of earlier couple stress theories (Mindlin, Tiersten, 1962; Koiter, 1969; Toupin, 1962; Voigt, 1887; Cosserat, Cosserat, 1970; Yang *et al.*, 2002) by introducing skew-symmetric couple stress tensor and refined couple stress coefficient ($\eta = \mu l^2$) determined by bulk modulus (μ) and characteristic length of the material (l). Skew-symmetric couple stress tensor captures internal rotations and moment stresses while characteristic length scale parameter enables to study size-dependent effects and microstructural interactions. Development of size-dependent couple stress theory in Timoshenko beams results in an increased stiffness predictions compared to classical beam theories, highlighting the importance of size effects in structural analysis (Asghari *et al.*, 2011). Dargush, *et al.* (2021) conducted two-and three-dimensional elastostatic analysis applying Ritz variational approach within the framework of size-dependent couple stress theory.

Several studies have also examined wave propagation in micro-structured plates using CCST models, focusing primarily on size-dependent effects and couple-stress elasticity. Ghodrati et al (2018) applied CCST to study the lamb waves propagation considering microstructure effects in very high frequencies. Huang *et al.* (2024) analysed Lamb waves in micro/nano-plates subjected to CCST . Their findings show that in anti-symmetric modes, the plate surface exhibits no in-plane displacement while at specific frequencies on the intersection points of symmetric and anti-symmetric dispersion curves out-of-plane displacement vanishes on the free surface. Wu and Hsu (2022) observed the mechanical behavior of functionally graded microplate accounting for size effects using the consistent couple stress theory. Sharma and Kumar (2015) not only studied the lamb waves in plate with the liquid loadings but also investigated the effects of rotation and thermal parameters on both plane and Rayleigh waves using CCST (Sharma, Kumar, 2023). Wu and Hu, (2021) proposed a unified size-dependent plate theory for static bending and free vibration analyses of micro- and nano-scale plates using the consistent couple stress theory.

The consistent couple stress theory (CCST) has been extensively utilized in various structural analyses (Wang *et al.*, 2017; Kaur *et al.*, 2024; Deep, Sharma, 2023; Sharma, Kumar, 2014), its application to shear-horizontal (SH) wave propagation in plates remains a relatively unexplored domain. The present study introduces a novel investigation into the propagation behavior of SH waves in a rotating microstructural plate subjected to elastically restrained boundary conditions (ERBC). The formulation employs CCST, which incorporates a characteristic length parameter linking the macroscopic response of the material to its intrinsic microstructure, thereby enhancing accuracy for micro- and meso-scale applications. Furthermore, the inclusion of additional terms in the equations of motion, corresponding to centripetal and coriolis effects, enables a more realistic representation of rotational influences. Elastically restrained boundary conditions, which interpolate between fully stress-free and fully clamped states, are critical for accurately modeling the behavior of plates in practical engineering systems. Comprehensive graphical analyses are presented to illustrate the effects of microstructural parameters, characteristic length, plate thickness, and boundary conditions on phase velocity under rotational

motion. The outcomes are compared with non-rotating cases, providing useful insights into the influence of rotation on wave behavior. These findings may have potential relevance to a broad range of engineering applications, particularly in contexts where size-dependent effects and boundary constraints are significant.

2 Geometry and basic equations

Consider a thin micro-structured plate that is unbounded in the $x-$ and $z-$ directions and possesses a finite thickness of $2b$ along the $y-$ axis ($-\infty < x < \infty, -b \leq y \leq b, -\infty < z < \infty$). The Cartesian coordinate system has an origin O located at the geometric center of the plate, equidistant from its upper and lower boundaries. The positive $y-$ direction is taken vertically upward, through the thickness of the plate. The free surfaces of the plate are defined by the planes $y = b$ and $y = -b$. The medium (plate) is assumed to be rotating uniformly about an axis in the $x - y$ plane with angular velocity $\vec{\Omega} = (\Omega_1, \Omega_2, \Omega_3)$ and wave propagation is taken to travel along the $x-$direction.

For the two dimensional solution, all the physical quantities are supposed to be invariant along the $z-$direction, i.e., $\frac{\partial}{\partial z} \equiv 0$. The displacement vector $\vec{u}$ is expressed as $\vec{u} = (u(x, y, t), v(x, y, t), w(x, y, t))$, where u, v and w denotes the displacement components in the x, y and z directions respectively and t denotes time. According to the consistent couple stress theory, the equation of motion of a rotating body in the absence of body forces is given as (Schoenberg, Censor, 1973; Hadjesfandiari, Dargush, 2011)

$$(\lambda + \mu + \eta\nabla^2)\vec{\nabla}(\vec{\nabla} \cdot \vec{u}) + (\mu - \eta\nabla^2)\nabla^2\vec{u} = \rho\left[\frac{\partial^2\vec{u}}{\partial t^2} + \left(\vec{\Omega} \times \left(\vec{\Omega} \times \vec{u}\right)\right) + \left(2\vec{\Omega} \times \frac{\partial\vec{u}}{\partial t}\right)\right] \quad (1)$$

where $\vec{u} = (u, v, w)$ is displacement vector, λ and μ are Lame's constants, $\eta = \mu l^2$ is couple stress coefficient, l is characteristic length, ρ is density of material, $\vec{\Omega}$ is rotation vector and $\nabla^2 = \frac{\partial^2}{\partial x^2} + \frac{\partial^2}{\partial y^2} + \frac{\partial^2}{\partial z^2}$. The term $\vec{\Omega} \times \left(\vec{\Omega} \times \vec{u}\right)$ represents the centripetal acceleration resulting from time varying motion and the coriolis acceleration is denoted by the term $2\vec{\Omega} \times \frac{\partial\vec{u}}{\partial t}$.

The constitutive relations for consistent couple stress theory are given as

$$\sigma_{ji} = \lambda u_{k,k}\delta_{ij} + \mu(u_{i,j} + u_{j,i}) - \eta\nabla^2(u_{i,j} - u_{j,i}) \quad (2)$$

$$\mu_{ji} = 4\eta(\bar{\omega}_{i,j} - \bar{\omega}_{j,i}), \text{where } \bar{\omega}_i = \frac{1}{2}\epsilon_{ijk}u_{k,j} \quad (3)$$

where, σ_{ji} is force stress tensor, μ_{ji} is couple stress tensor, δ_{ij} is Kronecker's delta, ϵ_{ijk} is permutation tensor, $\bar{\omega}_i$ is rotation vector and $i, j, k = 1, 2, 3$.

3 Propagation of Shear Horizontal waves under rotation

Consider SH waves, propagating in a micro-structural plate under rotation. For the two-dimensional plate in the $x-y$ plane, the components of displacement and rotation are considered as $\vec{u} = (0, 0, w)$ and $\vec{\Omega} = (\Omega_1, \Omega_2, 0)$ respectively. Eq. (1) is transformed into the single partial differential equation as written below

$$C_2^2(1 - l^2\nabla^2)\nabla^2 w = \frac{\partial^2 w}{\partial t^2} - w(\Omega_1^2 + \Omega_2^2), \quad \text{where} \quad C_2 = \sqrt{\frac{\mu}{\rho}} \tag{4}$$

let the solution of Eq. (4) is assumed as

$$w = h(y)e^{i\xi(x-Ct)} \tag{5}$$

where $h(y)$ is the unknown function of y, ξ is a wave number, C is phase speed, $i = \sqrt{-1}$. On substituting Eq. (5) into (4), Eq. (4) reduces to the following fourth-order differential equations.

$$\frac{d^4h(y)}{dy^4} - \left(\frac{1}{l^2} + 2\xi^2\right)\frac{d^2h(y)}{dy^2} + \left(\xi^4 + \frac{\xi^2}{l^2}\left(1 - \frac{C^2}{C_2^2}\right) - \left(\frac{\Omega_1^2+\Omega_2^2}{C_2^2 l^2}\right)\right)h(y) = 0 \tag{6}$$

Solution of the above differential Eq. (6) is obtained as

$$h(y) = D_1 Cosh(R_1 y) + D_2 Sinh(R_1 y) + D_3 Cos(R_2 y) + D_4 Sin(R_2 y) \tag{7}$$

where D_1, D_2, D_3, D_4 are arbitrary constants and

$$R_1 = \sqrt{\xi^2 + \frac{1}{2l^2}\left(1 + \sqrt{1 + \frac{4\xi^2 C^2 l^2}{C_2^2} + \frac{4l^2}{C_2^2}(\Omega_1^2 + \Omega_2^2)}\right)}$$

$$R_2 = \sqrt{\frac{1}{2l^2}\left(\sqrt{1 + \frac{4\xi^2 C^2 l^2}{C_2^2} + \frac{4l^2}{C_2^2}(\Omega_1^2 + \Omega_2^2)} - 1\right) - \xi^2}$$

Thus, displacement component in Eq. (5) becomes

$$w(y) = \Big(D_1 Cosh(R_1 y) + D_2 Sinh(R_1 y) + D_3 Cos(R_2 y) + D_4 Sin(R_2 y) \Big) e^{i\xi(x-Ct)} \tag{8}$$

The non-zero component of stress and couple stress tensors are obtained as

$$\begin{aligned}\sigma_{yz} =&\mu\frac{\partial w}{\partial y} - \mu l^2\left(\frac{\partial^3 w}{\partial x^2\partial y} + \frac{\partial^3 w}{\partial y^3}\right)\\ =&\Big(\ D_1L_1Sinh(R_1y) + D_2L_1Cosh(R_1y) - D_3L_2Sin(R_2y) + D_4L_2Cos(R_2y)\ \Big)\, e^{i\xi(x-Ct)}\end{aligned} \tag{9}$$

$$\begin{aligned}\mu_{yx} =&2\mu l^2\left(\frac{\partial^2 w}{\partial x^2} + \frac{\partial^2 w}{\partial y^2}\right)\\ =&\Big(\ D_1L_3Cosh(R_1y) + D_2L_3Sinh(R_1y) - D_3L_4Cos(R_2y) - D_4L_4Sin(R_2y)\ \Big)\, e^{i\xi(x-Ct)}\end{aligned} \tag{10}$$

where $L_1 = \mu R_1 + \mu l^2\xi^2 R_1 - \mu l^2 R_1^3, L_2 = \mu R_2 + \mu l^2\xi^2 R_2 + \mu l^2 R_2^3, L_3 = 2\mu l^2(R_1^2 - \xi^2), L_4 = 2\mu l^2(R_2^2 + \xi^2)$.

4 Restrained boundary conditions

Elastically restrained boundary conditions (ERBC) can be conceptualized as boundary surfaces embedded with distributed springs. These springs simulate elastic restraints by imposing resistance to displacements and rotations. To incorporate restrained boundary conditions within a couple stress elastic model, it is necessary to account not only for the classical stress–strain relations but also for additional stiffness coefficients and couple stress effects. These coefficients govern the relationship between force stresses and displacements, as well as between couple stresses and rotation gradients. Consequently, such conditions permit limited displacement and rotation at the boundaries. Shear spring constant (k_1) representing resistance to tangential (shear) deformation while (k_2) represents the rotational spring constant, indicating resistance to rotational motion at the boundary. Here, *rotation* refers to the angular motion of the plate itself, and its influence is incorporated into the dispersion relation of shear-horizontal (SH) waves by accounting for coriolis and centrifugal forces within the framework of rotating couple stress theory. For SH wave propagation, the tangential and rotational stiffness coefficients respectively characterize the boundary's resistance to tangential displacement and rotational deformation. Boundary conditions at the two surfaces ($y = \pm b$) of the plate are as follows (Mindlin, 1960; Wang *et al.*, 2017).

1) $\sigma_{yz} = k_1 w$
   This boundary condition leads to following equation in four unknown arbitrary constants
   $D_1L_1Sinh(R_1y)+D_2L_1Cosh(R_1y)-D_3L_2Sin(R_2y)+D_4L_2Cos(R_2y)-k_1D_1Cosh(R_1y)-k_1D_2Sinh(R_1y) - k_1D_3Cos(R_2y) - k_1D_4Sin(R_2y) = 0$

2) $\mu_{yx} = k_2\bar{\omega}_1,$ where $\bar{\omega}_1 = \frac{1}{2}\frac{\partial w}{\partial y}$
   This boundary condition yields the following equation in four unknown arbitrary constants
   $D_1L_3Cosh(R_1y)+D_2L_3Sinh(R_1y)-D_3L_4Cos(R_2y)-D_4L_4Sin(R_2y)-\frac{k_2}{2}D_1R_1Sinh(R_1y)-\frac{k_2}{2}D_2R_1Cosh(R_1y) + \frac{k_2}{2}D_3R_2Sin(R_2y) - \frac{k_2}{2}D_4Cos(R_2y) = 0$

where σ_{yz} is force stress, μ_{yx} is couple stress, w is displacement component, $\bar{\omega}_1$ is rotation vector, k_1, k_2 are tangential and rotational spring coefficients, respectively.

Enforcing the above boundary conditions at the plate boundaries ($y = \pm b$) leads to the following set of four homogeneous equations

$$\begin{pmatrix} D_1(L_1S_{11} - k_1C_{11}) + D_2(L_1C_{11} - k_1S_{11}) - \\ D_3(L_2S_{12} + k_1C_{12}) + D_4(L_2C_{12} - k_1S_{12}) \end{pmatrix} = 0 \tag{11}$$

$$\begin{pmatrix} D_1(-L_1S_{11} - k_1C_{11}) + D_2(L_1C_{11} + k_1S_{11}) - \\ D_3(-L_2S_{12} + k_1C_{12}) + D_4(L_2C_{12} + k_1S_{12}) \end{pmatrix} = 0 \tag{12}$$

$$\begin{pmatrix} D_1(L_3C_{11} - \frac{k_2}{2}R_1S_{11}) + D_2(L_3S_{11} - \frac{k_2}{2}R_1C_{11}) - \\ D_3(L_4C_{12} - \frac{k_2}{2}R_2S_{12}) - D_4(L_4S_{12} + \frac{k_2}{2}R_2C_{12}) \end{pmatrix} = 0 \tag{13}$$

$$\begin{pmatrix} D_1(L_3C_{11} + \frac{k_2}{2}R_1S_{11}) + D_2(-L_3S_{11} - \frac{k_2}{2}R_1C_{11}) - \\ D_3(L_4C_{12} + \frac{k_2}{2}R_2S_{12}) - D_4(-L_4S_{12} + \frac{k_2}{2}R_2C_{12}) \end{pmatrix} = 0 \tag{14}$$

here $S_{11} = Sinh(R_1b), S_{12} = Sin(R_2b), C_{11} = Cosh(R_1b), C_{12} = Cos(R_2b)$.

For the Eqs. (11-14) to possess the non-trivial solution, the determinant of unknown coefficients mush become zero.

$$|d_{ij}|_{4\times4} = 0 \tag{15}$$

where $d_{11} = -k_1C_{11}, d_{12} = L_1C_{11}, d_{13} = -k_1C_{12}, d_{14} = L_2C_{12}, d_{21} = L_1S_{11}, d_{22} = -k_1S_{11}, d_{23} = -L_2S_{12}, d_{24} = -k_1S_{12}, d_{31} = 2L_3C_{11}, d_{32} = -k_2R_1C_{11}, d_{33} = -2L_4C_{12}, d_{34} = -k_2R_2C_{12}, d_{41} = -k_2R_1S_{11}, d_{42} = 2L_3S_{11}, d_{43} = k_2R_2S_{12}, d_{44} = -2L_4S_{12}$

Solution of Eq. (15) gives the dispersion relation written below as

$$PX^2 + QX - P = 0 \tag{16}$$

where $X = \frac{tanh(R_1b)}{tan(R_2b)}$, $P = 2k_1k_2(L_2L_4R_1 - L_1L_3R_2) + k_1^2k_2^2R_1R_2 - 4L_1L_2L_3L_4$,
$Q = (k_1^2 - L_1^2)(k_2^2R_2^2 + 4L_4^2) + (k_1^2 + L_2^2)(-k_2^2R_1^2 + 4L_3^2) + 8k_1^2L_3L_4 - 4k_1k_2(L_2L_3R_2 + L_1L_4R_1)$

The analysis of Eq. (16) leads to the derivation of two distinct dispersion relations associated with SH waves

$$\frac{tanh(R_1b)}{tan(R_2b)} = \frac{-Q - \sqrt{Q^2 + 4P^2}}{2P} \tag{17}$$

$$\frac{tanh(R_1b)}{tan(R_2b)} = \frac{-Q + \sqrt{Q^2 + 4P^2}}{2P} \tag{18}$$

5 Modes of SH waves

The dispersion relation (16) comprises both symmetric and anti-symmetric components. Since, Eqs. (17) and (18) are reduced forms of Eq. (16), it is pertinent to examine which of these equations corresponds to the symmetric or anti-symmetric modes.

Let the restraint parameters in the boundary conditions be relaxed *i.e.* $k_1 = k_2 = 0$. Consequently, the boundary conditions discussed in the section (4) simplify to $\sigma_{yz} = 0,\ \mu_{yx} = 0$, corresponding to stress-free boundary conditions. Under these conditions, Eq. (15) reduces to the following two distinct dispersion relations for SH waves respectively.

$$\frac{tanh(R_1 b)}{tan(R_2 b)} = \frac{L_2 L_3}{L_1 L_4} \tag{19}$$

$$\frac{tanh(R_1 b)}{tan(R_2 b)} = \frac{-L_1 L_4}{L_2 L_3} \tag{20}$$

By imposing the symmetric conditions ($D_2 = D_4 = 0$) and anti-symmetric conditions ($D_1 = D_3 = 0$) as in (Yu and Yu, 1996) on Eqs. (11-14), the derived Eqs. (19) and (20) are directly obtained for the stress-free case. Accordingly, Eqs. (17) and (18) can be identified as representing the symmetric and anti-symmetric modes of SH waves.

6 The special cases

For stress-free boundary conditions, the surface tractions vanish, whereas rigid surface boundary conditions enforce zero displacements at the surface. Elastically restrained boundary conditions provide a transition between stress-free and rigid boundary conditions by introducing finite stiffness at the boundary. These three boundary conditions are discussed in this section.

Case:1 Stress-free boundary conditions

Stress free boundary conditions are achieved by specifying $k_1 = k_2 = 0$ in the boundary conditions discussed in section (4). Upon using these conditions in Eqs. (11-14), two dispersion relations (19) and (20) are attained in section (5) which are same as discussed by Sharma and Kumar (2023).

Case:2 Mixed boundary conditions

In the boundary conditions mentioned in the section (4), if $k_1 \to \infty$ and $k_2 = 0$, then the conditions become $w = 0, \mu_{yx} = 0$. Thus, the solution of the determinant in Eq. (15) produces two dispersion relations for the SH waves

$$Cosh(R_1 b)\ Cos(R_2 b) = 0 \tag{21}$$

$$Sinh(R_1 b)\ Sin(R_2 b) = 0 \tag{22}$$

Using the above mentioned mixed boundary conditions, the Eqs. (21) and (22) can also be derived from the Eqs. (17) and (18). Thus, Eqs. (21) and (22) can be classified as symmetric

and anti-symmetric mode of vibrations of SH waves, respectively.

Case:3 Rigid boundary conditions

In rigidly fixed boundary conditions, both displacement and rotation are totally restricted at the boundary. Thus, in this case $w = 0,\ \bar{\omega}_1 = 0$, obtained by putting $k_1 \to \infty, k_2 \to \infty$ in the boundary conditions stated in section (4). The determinant in Eq. (15) reduces to the following two distinct dispersion relations

$$\frac{tanh(R_1 b)}{tan(R_2 b)} = \frac{-R_2}{R_1} \tag{23}$$

$$\frac{tanh(R_1 b)}{tan(R_2 b)} = \frac{R_1}{R_2} \tag{24}$$

On the basis of the discussion in the case 1 and case 2 regarding obtaining dispersion relations directly by using these conditions in Eqs. (17) and (18), we can group Eqs. (23) and (24) to as symmetric and anti-symmetric modes of vibrations of SH waves in a micro-structural plate subject to rigid boundary conditions.

7 Verification and comparative analysis of the model

7.1 Assessment of model consistency with classical theory

Within the framework of Consistent Couple Stress Theory (CCST), stress-strain behavior of a material is governed not only by the classical continuum parameters but also by an intrinsic material length scale parameter (l). This quantitatively characterizes size-dependent behavior resulting from the material's micro-structural effects.

In the vanishing length scale limit ($l \to 0$), higher order couple stress effects are suppressed. The differential equation (6) reduces to the following differential equation of second order

$$\frac{d^2 h(y)}{dy^2} - \left(\xi^2 \left(1 - \frac{C^2}{C_2^2}\right) - \left(\frac{\Omega_1^2 + \Omega_2^2}{C_2^2}\right)\right) h(y) = 0 \tag{25}$$

Solution of Eq. (25) will be

$$h(y) = E_1 cos(\beta y) + E_2 sin(\beta y)$$

and thus

$$w(y) = \left(E_1 cos(\beta y) + E_2 sin(\beta y)\right) e^{i\xi(x - Ct)} \tag{26}$$

where E_1, E_2 are arbitrary constants and $\beta^2 = \frac{\Omega_1^2 + \Omega_2^2}{C_2^2} - \xi^2 \left(1 - \frac{C^2}{C_2^2}\right)$.

The restrained boundary condition in section (4) simplifies to $\sigma_{yz} = k_1 w$. Applying this condition at the two surfaces ($y = \pm b$) of the plate, following pair of homogeneous equations are obtained

$$E_1(-k_1) cos(\beta b) + E_2(\mu\beta) cos(\beta b) = 0 \tag{27}$$

$$E_1(\mu\beta)sin(\beta b) - E_2(k_1)sin(\beta b) = 0 \tag{28}$$

Enforcing a non-trivial solution for Eqs. (27) and (28) leads to the following equation

$$\left(k_1^2 - (\mu\beta)^2\right) sin(\beta b)cos(\beta b) = 0 \tag{29}$$

Eq. (29) is the dispersion relation for the propagation of SH waves in a micro-structured rotating plate with restrained boundary condition.

On assuming the tangential spring coefficient (k_1) to be zero, the boundary condition becomes $\sigma_{yz} = 0$. Thus, Eq. (29) reduces to $sin(\beta b)cos(\beta b) = 0$, which can be further simplified to the resulting pair of dispersion relations

$$sin(\beta b) = 0, \quad i.e., \quad \beta b = \frac{n\pi}{2}, \quad n = 0, 2, 4... \tag{30}$$

$$cos(\beta b) = 0, \quad i.e., \quad \beta b = \frac{n\pi}{2}, \quad n = 1, 3, 5... \tag{31}$$

Here, β is still having the rotational term in it. Thus, Eqs. (30) and (31) correspond to the symmetric and anti-symmetric modes of SH wave, respectively, in a rotating plate under classical theory of elasticity.

Furthermore, in the absence of rotation ($\Omega_1 = \Omega_2 = 0$), one obtains $\beta = \xi^2 \left(\frac{C^2}{C_2^2} - 1\right)$. In this case, Eqs. (30) and (31) represent the symmetric and anti-symmetric modes of SH wave, respectively, in an elastic plate as derived in Graff (2012). This confirms that the proposed model is consistent with classical elasticity theory and accurately reproduces the conventional behavior in the absence of micro-structural effects, rotational influences and restrained coefficients, thereby validating the formulation.

7.2 Comparison with the existing studies

A review of the literature indicates that numerous studies have examined the propagation of various elastic waves, investigating the influence of factors such as micro-structural parameter, rotation, stiffness, and boundary conditions in different elastic media. However, when focus is restricted to plate structures, the available research remains comparatively limited. The present study investigates the combined effects of rotation, length scale parameter and elastically restrained boundary conditions (ERBC) on SH wave propagating in an elastic plate within the framework of CCST theory. This section presents a comparison of the proposed model with existing studies, as summarized in Table 1, along with relevant references.

Table 1: Comaprison of present model with existing studies

Model	**Rotation**	**Characteristic length**	**ERBC**	**Problem type**	**Relevant References**
Classical Elasticity	✗	✗	✗	SH waves in plate	Graff(2012) Kuznetsov(2006)
	✓	✗	✗	Reflection and refraction of plane waves	Schoenberg, Censor(1973); Censor, Schoenberg(1973)
CCST	✗	✓	✗	Lamb waves in plate	Sharma and Kumar(2014)
	✗	✓	✗	SH waves in coupled plates	Dua and Sharma(2024)
	✗	✗	✓	waves in elastic media	Moukhomodiarov et al (2012); Moukhomodiarov andRogerson (2012)
	✗	✓	✗	SH waves in plate	Sharma and Kumar(2023)
	✓	✓	✓	Reflection and refraction of plane waves	Wang et al (2017)
	✓	✓	✓	SH waves in plate	Present study

8 Numerical results and discussion

SH waves in a plate display multimodal behavior along with dispersion characteristics. One notable aspect of this study involves the combined effect of rotation and stiffness coefficients on the phase velocity dispersion. For graphical illustration of the results, the material parameters are taken (Wang *et al.*, 2017) as $\lambda = 2.2\times10^{10}\ N/m^2, \mu = 1.1\times10^{10}\ N/m^2, \rho = 2.6\times10^3\ kg/m^3$. The standard values of stiffness constants are $k_1 = 10^{16}\ N/m^3$ and $k_2 = 10^4\ N/m$.

The characteristic length is chosen to be of the same order as the plate thickness $l \sim b$ to capture size-dependent effects. The stiffness parameters range from zero (stress-free) to infinity (perfectly constrained); however, finite values are adopted to represent realistic surface conditions in line with established literature. The rotational speed ($10^8\ rad/sec$) though high for macroscopic systems, is appropriate for micro/nano-scale devices and enables capturing rotational effects on wave propagation. Moreover, to address this, dimensionless parameters have also been introduced. Since, similar behavior is observed in both symmetric and anti-symmetric modes, the graphs are presented only for the symmetric cases.

8.1 Symmetric and anti-symmetric modes of SH waves

The dispersion relation expressed in Eq. (16), derived in section (4) reduces to two distinct forms as presented in Eqs. (17) and (18). These two relations correspond respectively to the symmetric and anti-symmetric cases of propagation, consistent with the classification outlined in section (5). Figures (1) and (2) depict the variation of non dimensional phase velocity with respect to the non dimensional wavenumber for both cases, highlighting the influence of the rotational parameter. These figures plot the non dimensional phase velocity against non dimensional wavenumber for mode numbers, $n = 1, 2, 3$. These profiles clearly show two robust features. First, for both the non-rotating and rotating cases the phase-velocity curves for successive mode numbers are shifted upward (higher modes propagate with higher phase velocity for a given non dimensional wave number), indicating the classical higher-mode stiffening. Second, the introduction of rotation systematically reduces the phase velocity of every mode. This reflects the additional effective inertia introduced by rotation (rotational inertia and coriolis-type coupling) mitigates the stiffening effect associated with couple stress. A modal asymmetry is also evident: the symmetric branch does not admit a fundamental (low-frequency) propagating mode under the present couple-stress boundary conditions, whereas the anti-symmetric branch supports a fundamental mode that exhibits a trend opposite to that of the higher anti-symmetric branches and is characterized by a cutoff frequency/wavenumber, below which wave propagation does not occurs. The cutoff and the reversed low-frequency trend are controlled by the non-dimensional characteristic length and the rotational parameter, demonstrating a sensitive competition between microstructural stiffening and rotational softening.

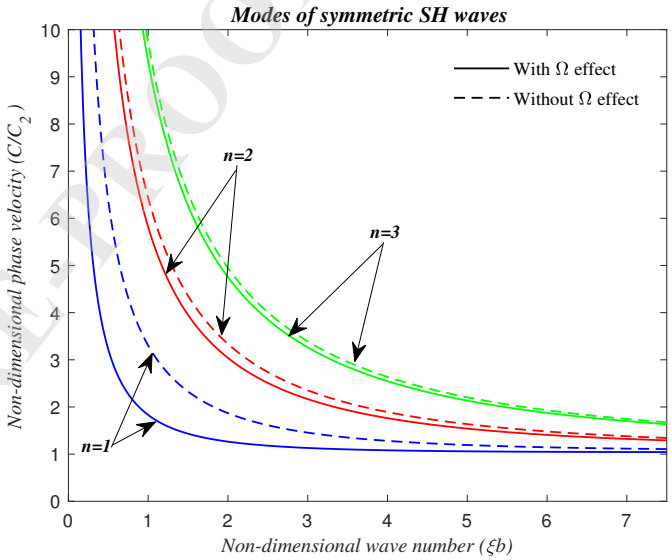

Figure 1: Phase velocity profiles for illustrating modes of symmetric SH waves

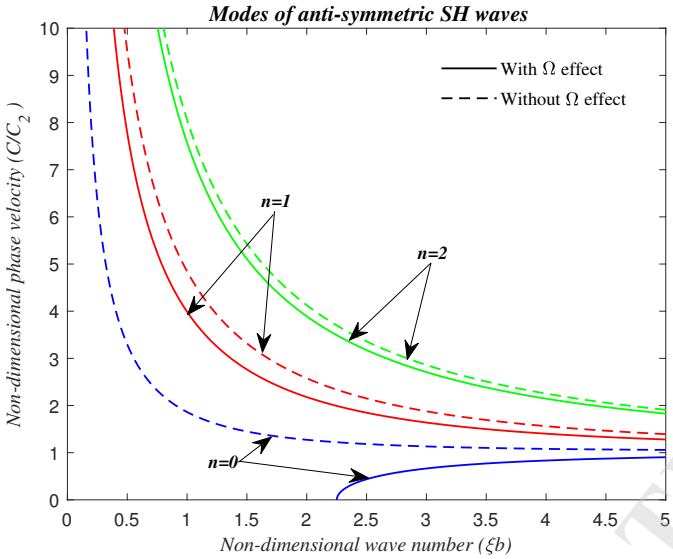

Figure 2: Phase velocity profiles for illustrating modes of anti-symmetric SH waves

8.2 Effect of dimensionless rotation parameter (Ω_2^*)

In a rotating couple-stress elastic medium, the propagation of SH waves is strongly influenced by the inertial effects associated with the rotational components, which directly modify the governing equations of motion and thereby alter the dispersion characteristics. The two components of the rotation vector, Ω_1 and Ω_2, appear in the governing relations through their sum of squares, $\Omega_1^2 + \Omega_2^2$, as evident from the values of R_1 and R_2 in section-3

Dimensionless parameters play a crucial role in characterizing wave propagation behavior by encapsulating the combined effects of material properties and characteristic length scales. In particular, $\Omega_2^* = (\Omega_2 l)/C_2$ quantifies the relative influence of characteristic length, rotation and shear wave velocity. Accordingly, the dispersion behavior of symmetric and anti-symmetric SH waves is examined under varying values of Ω_2^*. Figure (3) shows that for a fixed wave number (ξb), an increase in the value of Ω_2^* leads to the systematic reduction in phase velocity. This effect is more pronounced at smaller wave numbers. The significant variation in phase velocity at small wave numbers reflects strong dispersive effects that progressively diminish as (ξb) increases. At large wave numbers, the dispersion curves coalesce due to the diminishing influence of coupling and micro-structural effects.

Since, Ω_1 and Ω_2 enter the governing equations through the combined quadratic form $\Omega_1^2 + \Omega_2^2$; consequently, dimensionless rotation parameter Ω_1^* contributes identically to the phase velocity of SH waves.

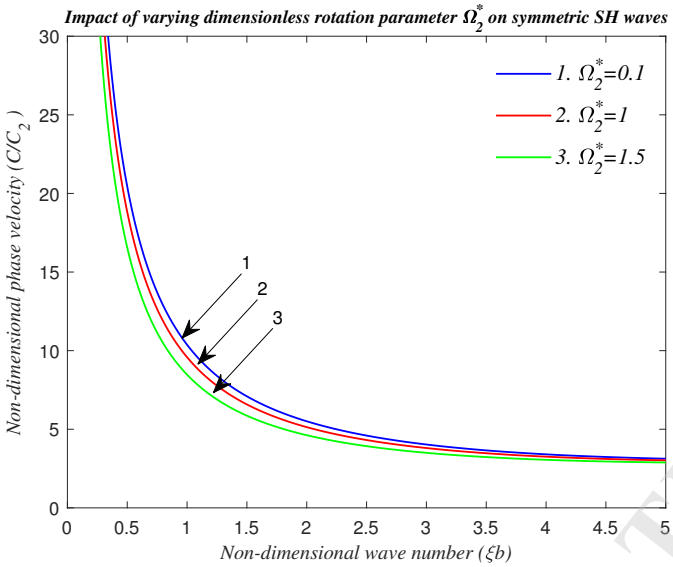

Figure 3: Phase velocity profiles for illustrating impact of dimensionless rotation parameter Ω_2^* on symmetric SH waves

8.3 Effects of plate thickness

Geometric parameters play a crucial role in determining the propagation characteristics of waves in solid media. In the present case, the finite thickness of the plate governs the boundary conditions and, consequently, the modal structure of the SH waves. Figure (4) illustrates the variation of non dimensional phase velocity with respect to non- dimensional wavenumber for different plate thicknesses.

It is observed that the phase velocity exhibits a negative correlation with plate thickness, whereby as the thickness increases, the phase velocity decreases. Both the non-rotating and rotating cases display this decreasing trend. However, when rotation is incorporated, the phase velocity profiles are slightly suppressed. Overall, the results emphasize that geometric scaling, in conjunction with rotational dynamics and couple stress effects, plays a decisive role in defining the dispersive response of SH waves in finite plates. Increasing plate thickness tends to reduce the phase velocity. Rotational effects further enhance this trend, leading to additional suppression of wave propagation.

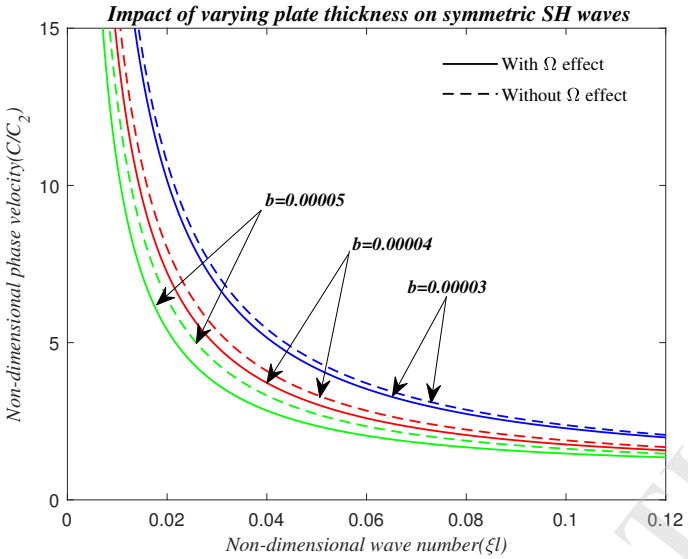

Figure 4: Phase velocity profiles for illustrating impact of varying plate thickness on symmetric SH waves

8.4 Effects of characteristic length parameter (l)

The characteristic length parameter (l) is a fundamental micro-structural quantity in couple stress elasticity, representing the internal material length scale or the average size of the microstructural cells. Typically of the order of 10^{-6} m, this parameter governs the extent to which micro-rotations and couple stresses influence the deformation field. To examine its impact on SH wave propagation under constrained plate conditions, phase velocity profiles were computed for different values of l. As shown in figure (5), an increase in the characteristic length parameter leads to a significant enhancement in phase velocity. This behavior can be attributed to the strengthening effect introduced by the microstructural interactions, which effectively increase the material's resistance to shear deformation. As l increases, the contribution of couple stresses to the total stress field becomes more dominant, resulting in an apparent stiffening of the medium and hence higher phase velocities. The trend clearly indicates that the internal length parameter acts as a stiffening factor, counteracting the dispersive softening associated with geometric and rotational effects. Consistent with earlier observations, the inclusion of rotational parameters slightly reduces the overall magnitude of phase velocity for each value of l. This demonstrates a competing interplay between microstructural stiffening (through l) and rotational softening (through Ω_1, Ω_2). At higher values of l, however, the microstructural effects tend to dominate, leading to comparatively higher phase velocity even in the presence of rotation.

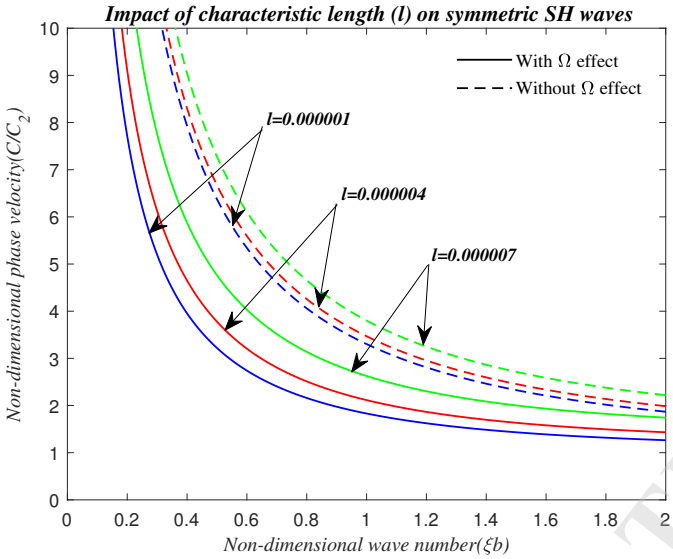

Figure 5: Phase velocity profiles for illustrating impact of varying characteristic length on symmetric SH waves

8.5 Effect of dimensionless parameters (l/b)

By analyzing the pronounced effects of the characteristic length scale and plate thickness on the dispersion behavior, the phase velocity is examined under rotational effects as a function of the dimensionless ratio l/b in figure (6). It is observed that increasing this ratio leads to a notable amplification of phase velocity, reflecting the enhanced resistance of the material to shear deformation. This effect is due to the additional stiffness contributed by microstructural effects. Proper consideration of the length-to-thickness ratio is therefore essential for accurately predicting deformation, natural frequencies, and stress distribution in microstructured or thin-scale structures.

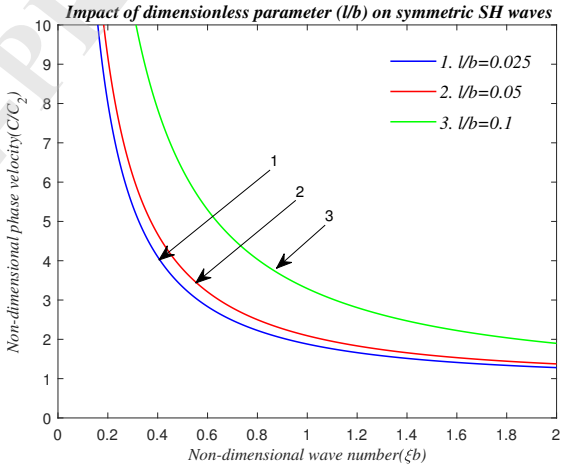

Figure 6: Phase velocity profiles for illustrating impact of dimensionless parameter l/b on symmetric SH waves

8.6 Effect of dimensionless stiffness parameters (k_1^* and k_2^*)

Wave propagation in microstructured solids are governed by both, the geometrical configuration and intrinsic physical properties. The introduction of dimensionless parameters $k_1^* = (k_1 l)/\mu$ and $k_2^* = k_2/(l\mu)$ consolidate the effects of material constant (μ), stiffness coefficients (k_1 and k_2) and the length scale parameter (l).

Figure (7) indicates that increasing k_1^* enhances the contribution of the material's microstructure, thereby increasing the effective shear stiffness of the plate and, consequently, the phase velocity. At constant wave number, profiles exhibit a direct relationship between the phase velocity and the dimensionless stiffness parameter, k_1^* . A pronounced dispersive effect is observed, particularly at short wavelengths, where the phase velocity exhibits a more rapid increase.

Contrary to the effect of k_1^*, the dimensionless quantity k_2^* in figure (8) is inversely related to the phase velocity. Higher values of k_2^* enhances the system's resistance to dynamic deformation and strongly constrain microrotations, consequently oppose wave propagation despite the apparent increase in boundary stiffness.

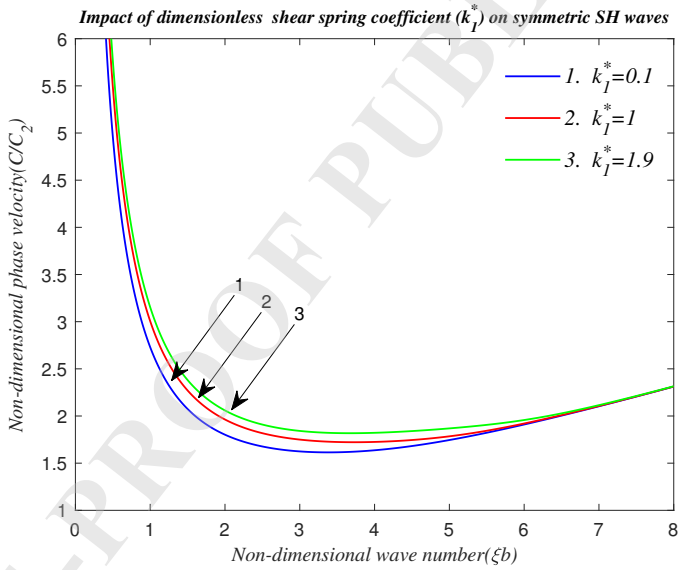

Figure 7: Phase velocity profiles for illustrating impact of dimensionless shear stiffness parameter (k_1^*) on symmetric SH waves

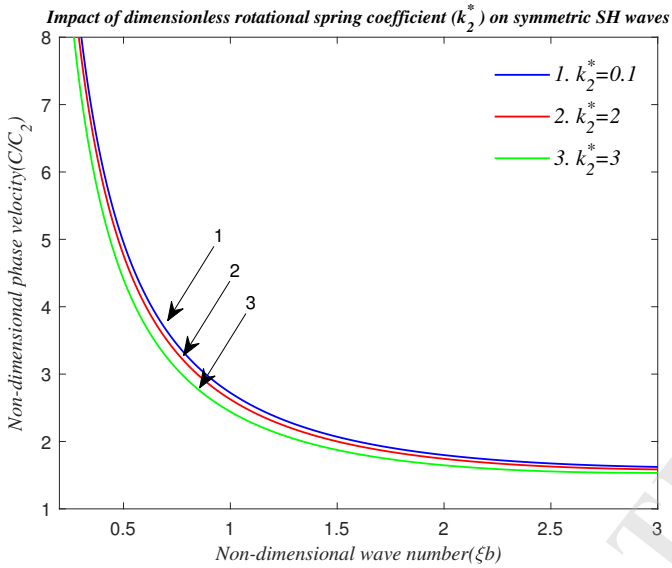

Figure 8: Phase velocity profiles for illustrating impact of dimensionless rotational stiffness parameter (k_2^*) on symmetric SH waves

8.7 Effect of boundary conditions

The dispersion relations labeled as $(19-20)$, $(21-22)$, and $(23-24)$ correspond to three distinct types of boundary conditions: stress-free, mixed, and fixed, respectively. These relations have been derived under both rotating and non-rotating conditions and are graphically represented in figures (9) and (10) for both symmetric and anti-symmetric shear-horizontal (SH) wave modes, respectively.

The stress-free boundary condition implies that both the normal and shear stress components at the boundary are zero, representing a completely traction-free surface (ideal for free surfaces like air-solid interfaces). The fixed boundary condition assumes zero displacement at the surface, meaning the boundary is perfectly clamped or rigidly constrained, often used to model bonding with rigid substrates. The mixed boundary condition represents an intermediate case where one stress component and one displacement component are set to zero. For example, tangential stress might be zero while normal displacement is constrained, modeling partial bonding or imperfect adhesion.

From the dispersion curves in figure (9), it is observed that for the symmetric mode of SH waves, the phase velocity corresponding to the stress-free boundary condition lies between those obtained for the mixed and fixed boundary conditions. In contrast, for the anti-symmetric mode shown in figure (10), a different ordering of phase velocity profiles is evident. In this case, the phase velocity is highest for the stress-free boundary condition and lowest for the mixed condition. Overall, the results indicate that the influence of boundary conditions on phase velocity is mode-dependent, leading to distinct trends for symmetric and anti-symmetric wave propagation.

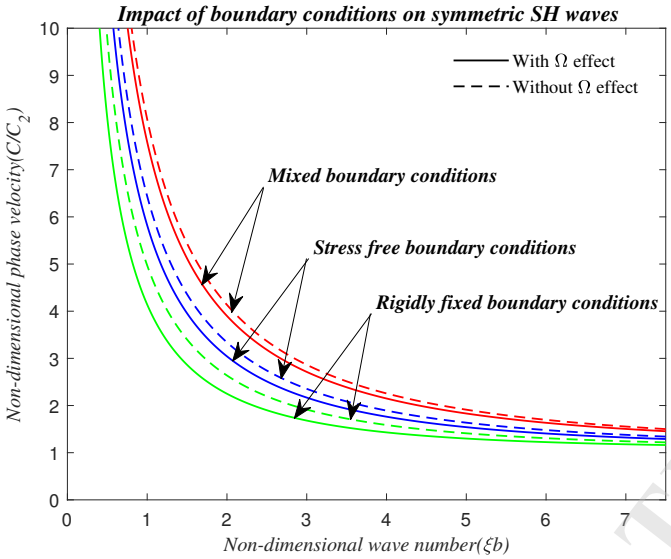

Figure 9: Phase velocity profiles for illustrating impact of boundary conditions on symmetric SH waves

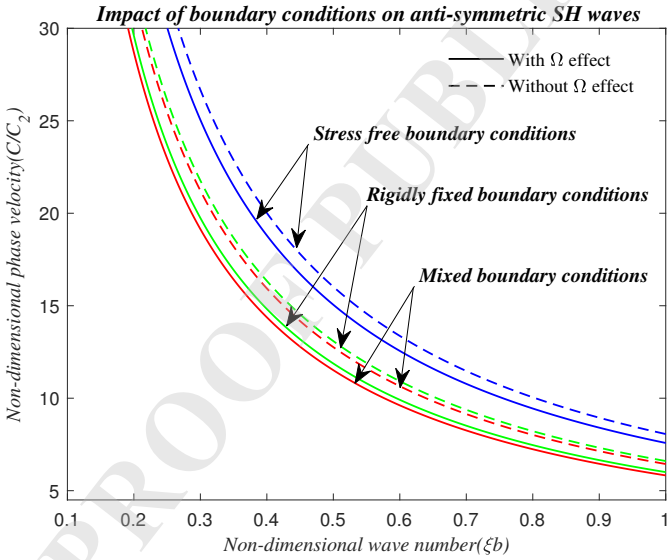

Figure 10: Phase velocity profiles for illustrating impact of boundary conditions on anti-symmetric SH waves

8.8 SH-wave propagation under different modeling assumptions

SH wave propagation in a micro-structured plate is governed by size-dependent effects, rotational motion, and boundary constraints, and the present model captures their combined influence. In the absence of rotation and boundary constraints, the formulation reduces to the CCST model, while further neglect of microstructural effects recovers the classical continuum model. The results show that the incorporation of the characteristic length parameter within the classical framework leads to an increase in phase velocity, as illustrated by curves 1 (present model), 2 (CCST), and 3 (classical) in figure (11). However, the inclusion of rotational effects reduce the phase velocity, resulting in the present model exhibiting an intermediate response between the classical and CCST predictions.

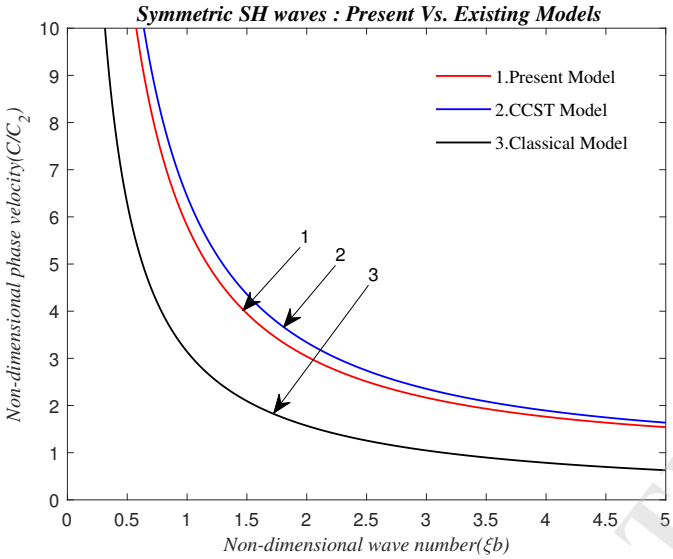

Figure 11: Phase velocity profiles for illustrating symmetric SH waves behavior under different models

9 Conclusion

The present study has thoroughly examined the dispersion behavior of shear-horizontal (SH) waves in a micro-structured couple stress elastic plate subjected to rotational effects induced by coriolis and centrifugal forces. The primary objective was to investigate the role of restrained boundary conditions, micro-structural and geometric features such as characteristic length and plate thickness as well as the dimensionless parameters on the wave propagation characteristics.

Plate rotation effects on SH wave modes: A detailed comparison between cases with and without plate rotation reveals that rotation leads to a consistent reduction in phase velocity across both symmetric and skew-symmetric SH wave modes. While symmetric modes exhibit minimal sensitivity, anti-symmetric modes show a more pronounced effect. Interestingly, the fundamental mode in skew-symmetric profiles undergoes a polarity reversal and exhibits a cut-off frequency, a distinct behavior not seen in non-rotating plates.

Role of dimensionless parameters, (Ω_1^* and Ω_2^*): The analysis indicates that both the rotation parameters (Ω_1^*) and (Ω_2^*) influence wave dispersion symmetrically due to the appearance of Ω_1 and Ω_2 as additive and squared terms in the governing equations. An increase in either dimensionless parameter leads to a decrease in phase velocity. This reduction is consistently observed in both symmetric and anti-symmetric SH wave modes.

Effect of plate thickness: The study reveals a clear inverse relationship between plate thickness and phase velocity, showing that an increase in thickness leads to a consistent reduction in phase velocity. This behavior highlights the sensitivity of wave propagation to geometric parameters, with plates of greater thickness exhibiting comparatively slower wave transmission.

Impact of characteristic length parameter (l)**:** As a core parameter of couple stress theory, the characteristic length significantly influences wave behavior. Increasing $'l'$ enhances phase velocity by amplifying micro-structural effects, thus enabling more efficient wave energy transmission. This effect highlights the importance of considering material length scales in micro-structured wave-guide designs.

Effect of dimensionless quantity, (l/b)**:** The results reveals that the phase velocity pattern is significantly influenced by variations in the ratio l/b. Changes in this parameter lead to noticeable modifications in the propagation characteristics of SH waves, highlighting the sensitivity of phase velocity to geometric scaling. An increase in l/b results in an amplification of phase velocity and enhanced dispersive behavior. This suggests that the structural configuration plays a crucial role in governing wave dynamics and is essential for optimizing design parameters in applications involving guided wave propagation.

Impact of dimensionless parameters, $(k_1^*$ **and** $k_2^*)$**:** The shear stiffness parameter (k_1) governs resistance to tangential deformation, whereas the rotational stiffness (k_2) regulates angular restraint. The phase velocity exhibits contrasting dependence on the non-dimensional parameters (k_1^*) and (k_2^*) Specifically, an increase in (k_1^*) leads to an increase in phase velocity, attributable to the enhanced stiffness that facilitates faster wave propagation. In contrast, an increase in (k_2^*) is associated with a reduction in phase velocity. Thus, these parameters influence wave speed in distinct ways and may be tuned to achieve desired propagation characteristics, as is often explored in wave-control technologies where analogous stiffness parameters are adjusted to tailor wave speed, attenuation, or confinement.

Implications of boundary conditions: The study also provides a comparative analysis of three different boundary condition types—stress-free, fixed, and mixed. By examining all three cases, the study highlights how boundary constraints can modify phase velocity profiles and wave behavior, providing insights into the sensitivity of wave propagation to edge conditions.

Assessment of SH wave propagation across different models: SH wave propagation in a microstructured plate is influenced by size-dependent effects, rotational motion, and boundary conditions, all of which are incorporated in the present model. The result shows that introducing a characteristic length scale increases phase velocity, while rotation decreases it, resulting in phase velocity curve of the present model to lie between classical theory and CCST predictions.

This analysis highlights the nuanced interplay between microstructure, boundary conditions, rotation, and geometric parameters in influencing the behavior of SH waves. The results contribute to a broader theoretical understanding of wave propagation in micro-structured rotating

plates and may offer useful guidance for design considerations in certain related engineering applications.

Fundings

This research did not receive any specific grant from funding agencies in the public, commercial, or not-for-profit sectors.

Conflict of interest

The authors declare that they have no known competing financial interests or personal relationships that could have appeared to influence the work reported in this paper.

Authors' contributions

All authors have contributed equally in the preparation of different sections of the manuscript.

Acknowledgments

The authors would like to deeply thank the editor and anonymous reviewers.

References

[1] Bhuta P.G., Jones J.P. (1963), Symmetric Planar Vibrations of a Rotating Disk, *Journal of the Acoustical Society of America*, **35**(7): 982–989, https://doi.org/10.1121/1.1918643.

[2] Schoenberg M., Censor D. (1973), Elastic waves in rotating media, *Quarterly of Applied Mathematics*, **31**(1):115–125, https://doi.org/10.1090/qam/99708.

[3] Censor D., Schoenberg M. (1973), Two-dimensional wave problems in rotating elastic media, *Applied Scientific Research*, **27**: 401–414, https://doi.org/10.1007/BF00382503.

[4] Advani S.H. (1967), Stationary waves in a thin spinning disk, *International Journal of Mechanical Sciences*, **9**(5):307–313, https://doi.org/10.1016/0020-7403(67)90023-9.

[5] Advani S.H., Bulkeley P.Z. (1969), Nonlinear transverse vibrations and waves in spinning membrane discs, *International Journal of Non-Linear Mechanics*, **4**(2):123–127, https://doi.org/10.1016/0020-7462(69)90021-3.

[6] Bulkeley P.Z. (1973), Stability of transverse waves in a spinning membrane disk, *Journal of Applied Mechanics*, **40**(1):133–136, https://doi.org/10.1115/1.3422911.

[7] Hashemi S.M., Richard M.J. (2001), Natural frequencies of rotating uniform beams with coriolis effects, *J. Vib. Acoust*, **123**(4):444–455, https://doi.org/10.1115/1.1383969.

[8] Huang Y.M., Wang C.-M. (2001), Combined methodology for analysis of rotary systems, *J. Vib. Acoust*, **123**(4):428-434, https://doi.org/10.1115/1.1385204.

[9] Lamb H., Southwell R.V. (1921), The vibrations of a spinning disk, *Proceedings of the Royal Society of London.Series A,containing papers of a Mathematical and Physical Character*, **99**(699):272–280, https://doi.org/10.1098/rspa.1921.0041.

[10] Luo A.C.J., Mote Jr. C.D. (2000), Nonlinear vibration of rotating thin disks, *J. Vib. Acoust*, **122**(4):376–383, https://doi.org/10.1115/1.1310363.

[11] Nowinski J.L. (1981), Stability of thermoelastic waves in membrane-like spinning disks, *Journal of Thermal Stresses*, **4**(1):1–11, https://doi.org/10.1080/01495738108909948.

[12] Southwell R.V. (1922), On the free transverse vibrations of a uniform circular disc clamped at its centre; and on the effects of rotation, *Proceedings of the Royal Society of London.Series A,containing papers of a Mathematical and Physical Character*, **101**(709):133–153, https://doi.org/10.1098/rspa.1922.0032.

[13] AuriaultJ.-L. (2004), Body wave propagation in rotating elastic media, *Mechanics research communications*, **31**(1):21–27, https://doi.org/10.1016/j.mechrescom.2003.07.002.

[14] Kumar R., Chawla V. (2011), Surface Wave Propagation in a Elastic Layer Lying Over a Generalized Thermodiffusive Elastic Half-Space with Imperfect Boundary, *Mechanics of Advanced Materials and Structures*, **18**(5):352-363, https://doi.org/10.1080/15376494.2010.517617.

[15] Yu Y.Y, Yu Y.Y. (1996), Linear Vibrations of Plates Based on Elasticity Theory, *Vibrations of elastic plates*, pp 31-55, https://doi.org/10.1007/978-1-4612-2338-2_2.

[16] Castaings M., Hosten B. (2001), Lamb and SH waves generated and detected by air-coupled ultrasonic transducers in composite material plates, *Ndt & E International*, **34**(4):249–258, https://doi.org/10.1016/S0963-8695(00)00065-7.

[17] Lee H., Jeon B., Cho Y. (2010), Damage detection in a plate using beam focused shear-horizontal wave magnetostrictive patch transducers, *AIAA journal*, **48**(3):654–663, https://doi.org/10.2514/1.44895.

[18] Kuznetsov S.V. (2022), On bifurcation of guided wave in functionally graded plates, *The European Physical Journal Plus*, **137**(10):1–9, https://doi.org/10.1140/epjp/s13360-022-03435-7.

[19] Kuznetsov S.V. (2006), SH-waves in laminated plates, *Quarterly of Applied Mathematics*, **64**(1):153–165, https://doi.org/10.1090/S0033-569X-06-00992-1.

[20] Phan H., cho Y., Pham C.V., Nguyen H., Bui T.Q. (2019), A theoretical approach for guided waves in layered structures, *In AIP Conference Proceedings*, **2102**:050011-1–050011-8

[21] Djeran-Maigre I., Kuznetsov S.V. (2014), Velocities, dispersion, and energy of SH-waves in anisotropic laminated plates, *Acoustical Physics*, **60**:200–207, https://doi.org/10.1134/S106377101402002X.

[22] Simonetti F., Cawley P. (2004), On the nature of shear horizontal wave propagation in elastic plates coated with viscoelastic materials, *Proceedings of the Royal Society of London.Series A:Mathematical,Physical and Engineering Sciences*, **460**(2048):2197–2221,

[23] Jiangong Y. (2011), Viscoelastic shear horizontal wave in graded and layered plates, *International journal of solids and structures*, **48**(16-17):2361–2372, https://doi.org/10.1016/j.ijsolstr.2011.04.011.

[24] Mindlin R.D. (1960), Waves and vibrations in isotropic, elastic plates, Structural mechanics, pp 199-232.

[25] Graff K.F. (2012), Waves motion in elastic solids, *Courier Corporation*.

[26] Moukhomodiarov R.R., Pichugin A.V., Rogerson G.A. (2010), The transition between Neumann and Dirichlet boundary conditions in isotropic elastic plates, *Mathematics and mechanics of solids*, **15**(4):462–490, https://doi.org/10.1177/1081286509103781.

[27] Moukhomodiarov R.R., Rogerson G.A. (2012), Long-wave dispersion phenomena in a layer subject to elastically restrained boundary conditions, *Zeitschrift für angewandte Mathematik und Physik*, **63**:171–188, https://doi.org/10.1007/s00033-011-0161-0.

[28] Moukhomodiarov R.R., Rogerson G.A. (2012), Generalisation of elastic models for a layer with elastically restrained boundaries, *International Journal of Engineering Science*, **57**:79–89, https://doi.org/10.1016/j.ijengsci.2012.04.004.

[29] Moukhomodiarov R.R., Rogerson G.A. (2013), Asymptotic long wave models for a pre-stressed elastic layer with elastically restrained boundaries, *International Journal of Solids and Structures*, **50**(11-12):1944–1953, https://doi.org/10.1016/j.ijsolstr.2013.02.014.

[30] Paimushin V.N., Gazizullin R.K. (2018), Acoustic Wave Propagation Through a Plate Fixed on a Rigid Frame Via Elastic Spacers and Located Between Two Barriers, *Journal of Applied Mechanics and Technical Physics*, **59**:733–746, https://doi.org/10.1134/S0021894418040211.

[31] Kuznetsov S.V. (2015), Lamb waves in a clamped and a partially clamped elastic layer, *Mechanics of Solids*, **50**:81–95, https://doi.org/10.3103/S0025654415010082.

[32] Hadjesfandiari A.R., Dargush G.F. (2011), Couple stress theory for solids, *International Journal of Solids and Structures*, **48**(18):2496–2510, https://doi.org/10.1016/j.ijsolstr.2011.05.002.

[33] Mindlin R.D., Tiersten H.F. (1962), Effects of couple-stresses in linear elasticity, *Archive for Rational Mechanics and Analysis*, **11**:415–448, https://doi.org/10.1007/BF00253946.

[34] Koiter W.T. (1969), Couple stresses in the theory of elasticity, I and II, *Philosophical Transactions of the Royal Society of London B*, **67**:17–44.

[35] Toupin R.A. (1962), Elastic materials with couple-stresses, *Archive for Rational Mechanics and Analysis*, **11**(1):385–414, https://doi.org/10.1007/BF00253945.

[36] Voigt W. (1887), Theoretical studies of the elastic behaviour of crystals, *Presented at the session of the Royal Society of Science on 2 July 1887.*

[37] Cosserat E., Cosserat F. (1909), *Theory of deformable bodies*, National Aeronautics and Space administration, Washington, D.C.

[38] Yang F., Chong A.C.M., Lam D.C.C., Tong P. (2002), Couple stress based strain gradient theory for elasticity, *International journal of solids and structures*, **39**(10):2731–2743, https://doi.org/10.1016/S0020-7683(02)00152-X.

[39] Asghari M., kahrobaiyan M.H., Rahaeifard M., Ahmadian M.T. (2011), Investigation of the size effects in Timoshenko beams based on the couple stress theory, *Archive of Applied Mechanics*, **81**:863–874, https://doi.org/10.1007/s00419-010-0452-5.

[40] Huang H., Guan W., He X. (2024), Modal displacement analyses of Lamb waves in micro/nano-plates based on the consistent couple stress theory, *ultrasonics*, **138**:107272, https://doi.org/10.1016/j.ultras.2024.107272.

[41] Wu C.-P., Hsu C.-H. (2022), A three-dimensional weak formulation for stress, deformation, and free vibration analyses of functionally graded microscale plates based on the consistent couple stress theory, *Composite Structures*, **296**:115829, https://doi.org/10.1016/j.compstruct.2022.115829.

[42] Dargush G.F., Apostolakis G., Hadjesfandiari A.R. (2021), Two-and three-dimensional size-dependent couple stress response using a displacement-based variational method, *European Journal of Mechanics-A/Solids*, **88**:104268, https://doi.org/10.1016/j.euromechsol.2021.104268.

[43] sharma V., Kumar S. (2015), Effects of liquid loadings on lamb waves in context of size dependent couple stress theory, *Journal of Theoretical and Applied Mechanics*, **53**(4):925–934, http://dx.doi.org/10.15632/jtam-pl.53.4.925.

[44] sharma V., Kumar S. (2023), A study of plane and Rayleigh waves in a microstructural medium: the role of size dependency and thermal effects, *Mechanics of Solids*, **58**:1335-1350, https://doi.org/10.3103/S0025654423600599.

[45] Wu C.-P., Hu H.-X. (2021), A unified size-dependent plate theory for static bending and free vibration analyses of micro- and nano-scale plates based on the consistent couple stress theory, *mechanics of Materials*, **162**:104085, https://doi.org/10.1016/j.mechmat.2021.104085.

[46] Wang C., Chen X., Wei P., Li Y. (2017), Reflection of elastic waves at the elastically supported boundary of a couple stress elastic half-space, *Acta Mechanica Solida Sinica*, **30**(2):154–164, https://doi.org/10.1016/j.camss.2017.03.004.

[47] Kaur M., Kumar S., Sharma V. (2024), Surface Waves in a Microstructural Couple Stress Half Space under the Extended Mindlin's Restrained Boundary Conditions, *Mechanics of Solids*, **59**(1):483–495, https://doi.org/10.1016/j.camss.2017.03.004.

[48] Deep S., Sharma V. (2023), Effects of microstructures, heterogeneity, and imperfectness on propagation of SH-waves in a fiber-reinforced layer sandwiched between two microstructural half-spaces, *Iranian Journal of Science and Technology, Transactions of Mechanical Engineering*, **47**:1161–1176, https://doi.org/10.1007/s40997-022-00570-5.

[49] Sharma V., Kumar S. (2023), A comprehensive analysis of horizontally polarized shear waves in a thin microstructural plate, *Structural Engineering and Mechanics, An Int'l Journal*, **85**(4):501–510, https://doi.org/10.12989/sem.2023.85.4.501.

[50] Sharma V., Kumar S. (2014), Velocity dispersion in an elastic plate with microstructure: effects of characteristic length in a couple stress model, *Meccanica*, **49**:1083–1090, https://doi.org/10.1007/s11012-013-9854-0.

[51] Dua N., Sharma V. (2024), Analysis of shear horizontal waves in heterogeneous/microstructural coupled plates: exploring the influence of interfacial bonding and the boundary conditions, *Journal of the Brazilian Society of Mechanical Sciences and Engineering*, **46**(11):643, https://doi.org/10.1007/s40430-024-05231-z.

[52] Ghodrati B., Yaghootian A., Ghanbar Zadeh A., Mohammad-Sedighi H. (2018), Lamb wave extraction of dispersion curves in micro/nano-plates using couple stress theories, *Waves in Random and Complex Media*, **28**(1):15–34, https://doi.org/10.1080/17455030.2017.1308582.